HHS Public Access

Author manuscript

Nat Neurosci. Author manuscript; available in PMC 2013 September 01.

Published in final edited form as:

Nat Neurosci. 2013 March ; 16(3): 332–339. doi:10.1038/nn.3322.

Experience-dependent modification of a central amygdala fear circuit

Haohong Li[1,*], **Mario A. Penzo**[1,*], **Hiroki Taniguchi**[1], **Charles D. Kopec**[2], **Z. Josh Huang**[1], and **Bo Li**[1,#]

[1]Cold Spring Harbor Laboratory, Cold Spring Harbor, NY 11724

[2]Department of Molecular Biology, Princeton University, Princeton, NJ 08544

Abstract

The amygdala is essential for fear learning and expression. The central amygdala (CeA), once viewed as a passive relay between the amygdala complex and downstream fear effectors, has emerged as an active participant in fear conditioning. However, how CeA contributes to the learning and expression of fear is unclear. Here we show in mice that fear conditioning induces robust plasticity of excitatory synapses onto inhibitory neurons in the lateral subdivision of CeA (CeL). This experience-dependent plasticity is cell-specific, bidirectional, and expressed presynaptically by inputs from the lateral amygdala. In particular, preventing synaptic potentiation onto somatostatin-positive neurons impairs fear memory formation. Furthermore, activation of these neurons is necessary for fear memory recall and sufficient to drive fear responses. Our findings support a model in which the fear conditioning-induced synaptic modifications in CeL favor the activation of somatostatin-positive neurons, which inhibit CeL output thereby disinhibiting the medial subdivision of CeA and releasing fear expression.

Extensive evidence indicates that the amygdala plays a central role in the learning and expression of conditioned fear[1–6]. It is well established that synaptic plasticity in the lateral amygdala (LA) is critical for the formation and storage of fear memory[7–13]. More recent studies recognize that the central amygdala (CeA) is another amygdala component actively involved in fear learning[14–19]. Indeed, pharmacological inactivation of CeA[14,16], or specific inactivation of the lateral subdivision of CeA (CeL)[17], during conditioning blocks the formation of fear memory. Moreover, fear conditioning induces changes in CeL neuronal activity, so that a population of cells ("CeL_{on}") becomes excited, while another ("CeL_{off}") inhibited in response to the conditioned stimulus (CS)[17–19]. These findings have led to the proposal that activity-dependent synaptic plasticity in CeL stores fear memory and underlies

#Correspondence: Bo Li, PhD, 1 Bungtown Road, Cold Spring Harbor NY 11724, bli@cshl.edu.

*These authors contributed equally to this work

Author Contributions

H.L. and M.A.P. performed the experiments. H.L., M.A.P., and B.L. analyzed data. H.T. and Z.J.H. provided critical reagents and advice. C.D.K. developed the MatLab programs for statistical (bootstrap) and behavioral analysis. H.L., M.A.P., and B.L. designed the study. B.L. wrote the manuscript.

The authors declare no competing financial interests.

the changes in cellular activity during fear conditioning. Nevertheless, fear conditioning-induced synaptic plasticity has not been observed in CeL.

If the presumed CeL synaptic plasticity stores fear memory, an important question is how the memory trace can be read out and translated into fear responses. The CeL, which is composed of several classes of GABA (γ-aminobutyric acid)-producing inhibitory neurons[6,18,20,21], gates fear expression by tonically inhibiting the medial subdivision of CeA (CeM)[17], the major output of amygdala[22]. Synaptic plasticity in distinct CeL cell populations, depending on their largely unknown connectivity, may play different roles in shaping CeL output, and therefore in controlling the function of CeM and the expression of fear[6].

In this study, we combined electrophysiological, optogenetic, and chemical-genetic methods to show that experience-dependent synaptic plasticity occurs and stores fear memory in the CeL inhibitory circuits following auditory Pavlovian fear conditioning. We further elucidated features of the functional organization of CeA inhibitory circuitry that allow this synaptic plasticity to serve as a link connecting fear learning and fear expression.

Experience-driven CeL synaptic plasticity

The GABA-producing inhibitory neurons in CeL can be classified based on the distinct neurochemical markers that they express[6,18,20,21]. Among these neurons, somatostatin-positive (SOM^+) neurons[21] constituted a major population and displayed heterogeneous electrophysiological properties (Fig. 1a, Supplementary Fig. 1)[23]. They were intermingled with SOM-negative (SOM^-) neurons, the majority of which expressed protein kinase C-δ ($PKC\text{-}\delta^+$) (Supplementary Fig. 1c). SOM^+ and $PKC\text{-}\delta^+$ neurons were largely non-overlapping (13 ± 1% of SOM^+ neurons expressed PKC-δ, n = 3 animals, mean ± s.e.m.), and may represent functionally distinct populations that play different roles in fear conditioning. Indeed, $PKC\text{-}\delta^+$ cells are mainly CeL_{off} neurons, and selective inhibition of these neurons facilitates fear conditioning[18].

To determine whether synaptic plasticity occurs in CeL in response to fear conditioning, we monitored excitatory synaptic transmission onto different classes of CeL neurons. We used a *SOM-IRES-Cre* knock-in mouse line, in which Cre is driven by the endogenous *SOM* promoter[24]. When crossed with the *Ai14* reporter mice[25], SOM^+ neurons in the resulting *SOM-IRES-Cre/Ai14* mice were readily identified by their red fluorescence (Fig. 1a). This strategy allowed us to examine synaptic transmission onto both the SOM^+ and SOM^- neurons in CeL.

We simultaneously recorded pairs of a SOM^+ (red fluorescent) and an adjacent SOM^-(non-fluorescent) neuron in the CeL in acute brain slices. Excitatory postsynaptic currents (EPSCs) were evoked by a stimulating electrode placed in the LA (Fig. 1b). Inputs from the basolateral amygdala (BLA), which also plays an important role in fear learning[26], may also be recruited by the stimulation. The critical advantage to this simultaneous paired-recording technique is that it allows the direct comparison of synaptic input strength onto two cells when stimulating the identical group of axons[27]. We measured the amplitude of the evoked

synaptic transmission onto both cells and computed its normalized values, which represent the true difference between cells in a pair (Fig. 1c; Supplementary Fig. 3).

In control animals, both AMPA receptor (AMPAR) and NMDA receptor (NMDAR) mediated EPSCs recorded from SOM^+ cells were significantly smaller than those from SOM^- neurons (Fig. 1c; Supplementary Fig. 3), indicating that the strength of excitatory synapses onto SOM^+ neurons is weaker than those onto SOM^- neurons under basal condition. Remarkably, in fear-conditioned animals, the strength of excitatory synapses onto these two populations of neurons, measured at either 3 hrs or 24 hrs after conditioning, was dramatically altered, such that AMPAR-mediated transmission onto SOM^+ neurons became much stronger than that onto SOM^- neurons (Fig. 1c; Supplementary Fig. 2; Supplementary Fig. 3). NMDAR-mediated transmission onto SOM^+ neurons was also enhanced relative to that onto the SOM^- neurons, albeit to a lesser extent.

The reversal of the relative strength of excitatory synaptic transmission onto SOM^+ versus SOM^- neurons following fear conditioning could be due to an increase in transmission onto SOM^+ neurons, a reduction of transmission onto SOM^- neurons, or a combination of both. To distinguish between these possibilities, we recorded miniature EPSCs (mEPSC; in the presence of tetrodotoxin to block action potentials and picrotoxin to block GABA-A-mediated synaptic currents) from both SOM^+ and SOM^- CeL neurons. Fear conditioning increased the frequency of mEPSCs recorded from SOM^+ CeL neurons at both 3 and 24 hrs following conditioning (Fig. 1d, e; Supplementary Fig. 2). It also increased the amplitude of mEPSCs in these neurons (Fig. 1e; Fig. 4d). In contrast, fear conditioning decreased the frequency of mEPSCs recorded from SOM^- CeL neurons, without appreciably affecting their amplitude (Fig. 1d, e) (mEPSC frequency: $F_{(2,71)} = 8.62$, $P < 0.001$, two-way analysis of variance (ANOVA); mEPSC amplitude: $F_{(2,71)} = 3.72$, $P < 0.05$, two-way ANOVA). These results demonstrate that fear conditioning strengthened the excitatory synapses onto SOM^+ neurons, while weakening those onto SOM^- neurons in the CeL.

To determine whether the synaptic modifications in CeL neurons occurred in synapses driven by inputs originating from, or axons passing through LA, we injected LA with an adeno-associated virus, AAV-CAG-ChR2(H134R)-YFP that expresses channelrhodopsin-2 (ChR2) which can activate neurons in response to light[28]. ChR2 was mainly expressed in LA neurons as a result of targeted viral injection (Fig. 2a, b). Excitatory synaptic transmission onto CeL neurons was reliably evoked by light (Fig. 2c, d), consistent with the existence of anatomical connection from LA to CeL[29]. In control animals, the light-evoked EPSCs in SOM^+ CeL neurons were much smaller than those in the simultaneously recorded SOM^- CeL neurons, however 24 hrs after fear-conditioning this relationship was reversed, so that the EPSCs in SOM^+ CeL neurons became larger (Fig. 2d, e; Supplementary Fig. 4; Supplementary Fig. 2). These results demonstrate that the fear conditioning-induced synaptic plasticity in CeL (Fig. 1) is located at synapses driven by the inputs from LA. On the other hand, ChR2 stimulation of axons originating from the auditory thalamus, another potential source of input to CeL[30,31], failed to evoke any detectable excitatory synaptic transmission onto CeL neurons, although it did evoke transmission onto LA neurons (Fig. 3). These results suggest that the fear conditioning-induced synaptic plasticity in CeL is in series with that in the LA[16].

To probe the nature of the fear conditioning-induced synaptic plasticity in the LA–CeL pathway, we employed a paired-pulse stimulation protocol using light to evoke transmission (Fig. 2c, d, and f). The paired pulse ratio (PPR), measured as the amplitude of the second EPSC relative to that of the first in response to the paired-pulse stimulation, reflects presynaptic release probability; lower PPR correlates with higher release probability[32]. In naïve animals, SOM^+ CeL neurons had higher PPR than SOM^- neurons (Fig. 2d, f). Interestingly, after fear conditioning, SOM^+ CeL neurons showed a marked decrease in PPR, whereas SOM^- neurons showed an increase (Fig. 2d, f). These results corroborate the changes in mEPSC frequency (Fig. 1d, e; Fig. 4c, d), and indicate that changes in presynaptic release probability can, at least in part, account for the fear conditioning-induced synaptic plasticity in CeL. Because fear conditioning also increased the amplitude of mEPSC in SOM^+ CeL neurons (Fig. 1e; Fig. 4d), an additional postsynaptic process likely contributes to the enhancement of excitatory synaptic transmission onto these neurons.

CeL synaptic potentiation stores memory

We wished to test whether the fear conditioning-induced synaptic plasticity in CeL is essential for the storage of fear memory. Synaptic plasticity, including both long-term potentiation (LTP) and long-term depression (LTD) of synaptic transmission, can be induced *in vitro* in CeL neurons[33,34] and is in general dependent on postsynaptic neuronal activation[35]. To specifically test whether the fear conditioning-induced synaptic strengthening onto SOM^+ CeL neurons is dependent on postsynaptic activity, and whether it is required for fear memory formation, we selectively suppressed SOM^+ neurons in CeL during learning by using a chemical-genetic method[36]. We bilaterally injected the CeL of *SOM-IRES-Cre* mice with an AAV-DIO-hM4Di-mCherry that expresses hM4Di, an engineered inhibitory G-protein coupled receptor that can suppress neuronal activity[36,37], in a Cre-dependent manner (Fig. 4a, b; Supplementary Fig. 5a, b). Two to three weeks after surgery, animals received treatment with CNO, the agonist of hM4Di, followed by fear conditioning (Fig. 4; Supplementary Fig. 5).

Selective suppression of SOM^+ CeL neurons by hM4Di during conditioning completely abolished the fear conditioning-induced synaptic strengthening (Fig. 4c, d, and compare them to Fig. 1d, e; Supplementary Fig. 2), and markedly impaired fear memory, which was measured as a reduction in the freezing behavior that is characteristic of fear[22], in response to the CS 24 hrs after conditioning (Fig. 4e; Supplementary Fig. 5c). Furthermore, the impairment of fear memory was significantly correlated with the extent of infection of SOM^+ CeL neurons with the AAV-DIO-hM4Di-mCherry (Fig. 4f). Importantly, hM4Di-mCherry was selectively expressed in the SOM^+ neurons in CeL (Fig. 4b; Supplementary Fig. 5a), and activation of hM4Di by CNO reversibly induced membrane hyperpolarization and suppressed neuronal firing (Supplementary Fig. 10 a, b). These results demonstrate that the fear conditioning-induced synaptic strengthening onto SOM^+ CeL neurons is dependent on postsynaptic activity, and that SOM^+ CeL neurons are required for fear learning. The most parsimonious explanation for these results is that the experience and activity-dependent strengthening of excitatory synapses onto SOM^+ CeL neurons (Fig. 1; Fig. 2; Fig. 4) is necessary for the formation and storage of fear memory.

The organization of CeA circuits

CeL tonically inhibits CeM[6,17–20,38], the main output nucleus of the amygdala[22], thereby gating the expression of fear[17,18]. To understand how the fear conditioning-induced modifications of CeL circuits can be read out and used to control fear expression, we examined the organization of CeA inhibitory circuitry. We injected the retrograde tracer cholera-toxin B (CTB) into CeM of *SOM-IRES-Cre/Ai14* mice (Fig. 5; Supplementary Fig. 6). CTB extensively labeled CeL neurons, revealing their direct projection to CeM (Fig. 5b, c). Notably, only 15.7 ± 3.8% of the CTB-labeled (green) neurons in CeL were SOM^+ (red) (Fig. 5c; similar results were obtained from 2 animals), indicating that the majority (~85%) of CeM-projecting neurons in CeL are SOM^- cells. This result is likely an overestimation of the contribution of SOM^+ neurons to the CeM-projecting cell population, because CTB can leak into CeL from the adjacent CeM. Consistent with the above observations, axonal fibers, which can be readily followed from neurons expressing ChR2-YFP, originating from SOM^+ CeL neurons occupied and filled the entire CeL, but not CeM (Fig. 6b; Supplementary Fig. 7b). These results suggest that the vast majority of SOM^+ CeL neurons do not directly inhibit CeM.

To directly assess the spatial range of SOM^+ CeL neuron-mediated inhibition, we crossed the *SOM-IRES-Cre* mice with the *Ai32* line, which expresses ChR2-YFP in a Cre-dependent manner[39]. In the resulting *SOM-IRES-Cre/Ai32* mice the ChR2-YFP was selectively and uniformly expressed in SOM^+ neurons (Fig. 6b). We focally stimulated SOM^+ neurons by shining light onto small areas, each of which was ~50 μm in diameter, within CeL in acute slices prepared from these mice (Fig. 6a–e). For each slice we systematically stimulated multiple areas that together covered the entire CeL (Fig. 4a, e). Inhibitory postsynaptic currents (IPSCs) in response to the light stimulation were recorded from neurons in either CeL or CeM in the same slice. Robust IPSCs were detected in all the recorded CeL neurons, including both SOM^+ neurons (identified by the expression of ChR2-YFP) and SOM^- neurons (identified by the lack of ChR2-YFP). Moreover, all CeL neurons responded to the stimulation of every CeL location (335 ± 93 pA, n = 17 cells, 3 animals, mean ± s.e.m; Fig. 6c, d). Consistent results were also obtained in a complementary experiment (Supplementary Fig. 7). These IPSCs were not driven by neurons from the LA or BLA, because SOM^+ neurons in these areas did not synapse onto CeL neurons (Supplementary Fig. 8). These results, together with the finding that PKC-δ^+ neurons, which are the major SOM^- neurons in CeL (Supplementary Fig. 1c), inhibit PKC-δ^- neurons[18], indicate that SOM^+ and SOM^- neurons in CeL mutually inhibit.

In contrast to the neurons in CeL, only 10% (4 out of 40) of randomly recorded neurons in the CeM showed detectable IPSCs, which were rather small (24 ± 9 pA, n = 4 cells, 3 animals, mean ± s.e.m; Fig. 6c), and these neurons did not respond to the stimulation of all CeL locations. Importantly, none (0 out of 16) of the retrogradely labeled periaqueductal gray (PAG)-projecting CeM neurons responded to the same stimulation with any measurable IPSCs (Fig. 6c, f). Thus, these results demonstrate that SOM^+ CeL neurons provide potent inhibition within CeL, however they do not appreciably inhibit CeM neurons. In particular, they do not inhibit the PAG-projecting CeM neurons. These results also indicate that SOM^+

and SOM$^-$ CeL neurons have different connectivity, because the PKC-δ$^+$ (and thus SOM$^-$) CeL neurons inhibit all the identified PAG-projecting CeM neurons[18].

SOM$^+$ CeL neurons control fear expression

It has been shown that pharmacological inhibition of CeL elicits freezing behavior through the disinhibition of CeM[17]. Our results so far indicate that SOM$^+$ CeL neurons can inhibit CeL output via local inhibition, and that they do not inhibit CeM neurons that project to PAG (Fig. 5; Fig. 6; Supplementary Fig. 7), the effector that triggers freezing behavior[22]. Based on these findings, we reasoned that activation of SOM$^+$ neurons might be sufficient to induce freezing behavior in naïve animals. To test this hypothesis, we selectively expressed ChR2 in SOM$^+$ neurons by injecting the AAV-DIO-ChR2(H134R)-YFP bilaterally into the CeL of *SOM-IRES-Cre* mice (Fig. 7a, b; also see Supplementary Fig. 7b). Optic fibers were implanted bilaterally into CeL to allow the activation of ChR2 in behaving animals with a blue laser (Fig. 7a)[40,41]. Light activation of SOM$^+$ neurons in CeL of naïve freely moving animals induced robust freezing that disappeared upon the cessation of light (Fig. 7c; Supplementary Movie 1), indicating that activation of SOM$^+$ neurons in CeL is sufficient to induce a fear-like response.

We reasoned that activation of SOM$^+$ CeL neurons might also mediate conditioned fear responses. This is because following fear conditioning, the strengthening of the excitatory synapses onto SOM$^+$ CeL neurons and the weakening of those onto SOM$^-$ CeL neurons alter the balance of excitation onto these two populations, favoring the activation of SOM$^+$ neurons in response to excitatory synaptic inputs (Fig. 1 and 2, Supplementary Fig. 3 and 4). Indeed, SOM$^+$ CeL neurons were preferentially activated in fear conditioned animals in response to CS, as measured by the expression of c-Fos (Supplementary Fig. 9), a marker for neuronal activation[42].

To test whether the activation of SOM$^+$ CeL neurons in fear conditioned animals is required for the expression of learned fear in response to CS presentations, we inhibited these neurons during fear memory recall. To achieve this goal, we selectively expressed Archaerhodopsin (Arch), the light-sensitive inhibitory proton pump[43] (Supplementary Fig. 10 c, d), in SOM$^+$ neurons by injecting the AAV-DIO-Arch-GFP bilaterally into CeL of *SOM-IRES-Cre* mice (Fig. 7a, d). Optic fibers were implanted bilaterally into CeL to allow the activation of Arch with a green laser (Fig. 7a). Animals were first fear conditioned and 24 hrs later tested for fear memory recall (Fig. 7e). Light-induced inhibition of SOM$^+$ neurons in CeL suppressed the conditioned freezing behavior, which was subsequently revealed upon the cessation of light (Fig. 7e; Supplementary Movie 2). These results together demonstrate that activation of SOM$^+$ neurons in CeL is not only sufficient to drive freezing behavior, but is also necessary for the expression of conditioned fear.

Discussion

Our study uncovers how the inhibitory circuits of CeL respond to fear conditioning and contributes to both the learning and expression of fear. Fear conditioning potentiated the excitatory synaptic transmission onto SOM$^+$ CeL neurons, while weakening that onto SOM$^-$

CeL neurons. These modifications occurred, largely through a presynaptic mechanism, in synapses driven by the inputs from LA. The opposing, cell-specific changes rendered the SOM^+ neurons more sensitive to excitatory synaptic inputs than SOM^- neurons, reversing the relationship found in naïve animals. Given that CeL neurons exhibited mutual inhibition, the fear conditioning-induced synaptic modifications bias the competition between mutually inhibitory CeL populations for excitatory inputs, so that SOM^+ neurons were preferentially activated. Once activated, SOM^+ neurons were sufficient to release fear responses, an outcome that is explained by the capacity of these neurons to inhibit CeL output while without inhibiting the PAG-projecting CeM neurons. These results are consistent with, and complement the finding that pharmacological inactivation of CeL disinhibits CeM and elicits freezing behavior[17].

Although fear conditioning modifies multiple synapses, the fear conditioning-induced potentiation of excitatory synaptic transmission onto SOM^+ CeL neurons appears to be crucial, as suppression of this potentiation severely impaired fear memory. The synaptic potentiation was detected at 3 hrs, and persisted for at least 24 hrs following fear conditioning, suggesting its involvement in both fear memory acquisition and consolidation[8]. Thus, our results support the notion that the experience-dependent strengthening of excitatory synapses onto SOM^+ CeL inhibitory neurons stores fear memory and enables the expression of conditioned fear.

Our results are consistent with a model in which CeA stores fear memory in series with LA[15–17]. Such serial organization of fear memory allows the regulation of fear conditioning at multiple levels. Moreover, as transmission is potentiated following fear conditioning, both at the auditory thalamus–LA synapses[44] and at the LA–CeL synapses (this study), the signal carrying CS information can be reliably transmitted from the auditory thalamus to CeA via LA while maintaining specificity. Parallel pathways may also participate in fear conditioning. For example, inputs from the brainstem parabrachial nucleus or the insula cortex to CeL may be recruited and play a role in fear conditioning.

Our findings delineate cellular and circuit mechanisms that may explain previously reported observations: 1) pharmacological inactivation of CeL during conditioning impairs fear learning[14,16,17]; 2) fear conditioning is followed by the appearance of two functionally distinct cell populations in CeL, the CeL_{on} and CeL_{off} neurons, which show opposite responses to CS[17–19]; and 3) the appearance of CeL_{on} neurons is associated with CeM activation, rather than inhibition[17]. Further studies will be required to elucidate the detailed cellular and molecular changes in distinct CeL inhibitory circuits during fear conditioning and to determine how they are related to fear memory acquisition, consolidation, and expression.

METHODS

Animals

Mice were group-housed under a 12-h light-dark cycle (9 a.m. to 9 p.m. light), with food and water freely available. Only animals with optic fiber implants were housed singly. The *SOM-IRES-Cre* mice and the *Rosa26-loxp-STOP-loxp-H2B-GFP* reporter line were

generated as described[24,45]. The *Ai14* reporter mice[25] and *Ai 32* mice[39] were purchased from The Jackson Laboratory. All mice were bred onto C57BL/6J genetic background. Male and female mice of 40–60 days of age were used for all the experiments. All procedures involving animals were approved by the Institute Animal Care and Use Committees of Cold Spring Harbor Laboratory and carried out in accordance with National Institutes of Health standards.

Immunohistochemistry

Immunohistochemistry experiments were performed following standard procedures[46]. Images were taken using a LSM 710 laser-scanning confocal microscope (Carl Zeiss). The primary antibodies used were: anti-PKC-δ (mouse or rabbit, Chemicon, 1:500), anti-somatostatin (rat, Millipore, 1:200; rabbit, Bachem, 1:2000), anti-GAD67 (mouse, Millipore, 1:800), and anti-c-Fos (rabbit, Santa Cruz, 1:2500).

Fear conditioning

Fear conditioning procedures were performed as previously described[47]. Briefly, mice were first handled and habituated to the conditioning cage and testing cage. Habituation and conditioning were performed, in separate days (Supplementary Fig. 2), in a Mouse Conditioning Cage (Test-A; 18 cm × 18 cm × 30 cm) with an electrifiable floor connected to a H13-15 shock generator (Coulbourn Instruments, Whitehall, PA). The Test-A cage was situated in a larger sound attenuated cabinet (H10-24A; Coulbourn Instruments). On Day1, mice were individually habituated in a Test-A cage with five pure tones (4-kHz, 75-dB, 30-s each) delivered at variable intervals (60–120 s). The entire duration of this session was 600 s. On Day 2, animals were conditioned, individually, using a similar protocol except that each of the five tones co-terminated with a 2-s 1-mA foot-shock (or 0.3 mA for experiments described in Fig. 4e, f). The FreezeFrame software (Coulbourn Instruments) was used to control the delivery of tones and foot-shocks. The floor and walls of the cage were cleaned with 70% ethanol for each animal. During habituation and conditioning the cabinet was illuminated and the behavior was captured with a monochrome CCD-camera (Panasonic WV-BP334) at 4 Hz and stored on a personal computer. The test for fear memory was performed in a testing cage, Test-B, in darkness 24 h after conditioning. Test-B (the testing cage) had a different shape (22 cm × 22 cm × 21 cm) and floor texture compared with Test-A (the conditioning cage). The floor and walls of Test-B were wiped with 0.5% acetic acid for each animal before testing to make the scent distinct from that of Test-A. Behavioral response to two 4-kHz 75-dB tone (the conditioned stimulus, CS) delivered with a 120 s interval was recorded. The entire duration of the test session was 340 s. Freezing behavior in response to the two CS presentations during the test session were scored and averaged. Freezing behavior was analyzed by using the FreezeFrame software (Coulbourn Instruments) or a MatLab (MathWorks, Natick, MA, USA)-based software[47], with the evaluator being blind to the treatment of the animals.

Stereotaxic surgery

All AAV viruses, such as the AAV-DIO-ChR2(H134R)-YFP, AAV-DIO-Arch-GFP, and AAV-DIO-hM4Di-mCherry, were produced by the University of North Carolina Vector

Core Facilities. The retrograde tracer Alexa-Fluor-488-conjugated cholera toxin (CTB) was purchased from Invitrogen. Standard surgical procedures were followed for stereotaxic injection[46]. Briefly, animals were anaesthetized with ketamine (100 mg/kg) supplemented with dexmedetomidine hydrochloride (0.4 mg/kg) and positioned in a stereotaxic injection frame (myNeuroLab.com). A digital mouse brain atlas was linked to the injection frame to guide the identification and targeting of CeL (Angle Two Stereotaxic System, myNeuroLab.com). CTB or viruses were delivered with a glass micropipette through a skull window (1–2 mm^2) by pressure application (5–12 psi, controlled by a Picrospritzer III, General Valve, Fairfield, NJ, USA). The injections were performed using the following stereotaxic coordinates for CeL: −1.22 mm from Bregma, 2.5 mm (4-week-old mice) or 2.9 mm (6–7-week-old mice) lateral from the midline, and 4.6 mm vertical from the cortical surface; for CeM: −1.00 mm from Bregma, 2.36 mm lateral from the midline, and 5.10 mm vertical from the cortical surface; for LA: −1.80 mm from Bregma, 3.4 mm lateral from the midline, and 4.9 mm vertical from the cortical surface; for auditory thalamus: −3.16 mm from Bregma, 1.90 mm lateral from the midline, and 3.20 mm vertical from the cortical surface; for PAG: −4.48 mm from Bregma, 0.36 mm lateral from the midline, and 2.60 mm vertical from the cortical surface. During all surgical procedures, animals were kept on a heating pad and were brought back to their home cages after regaining movement. For postoperative care, mice were hydrated by intraperitoneal injection with 0.3–0.5 ml of lactated ringers. We used metacam (meloxicam, 1–2 mg/kg) as an analgesic and to reduce inflammation. For the injection of CTB, we injected 0.1–0.3 μl (2% in PBS) into CeM and waited 3–5 days to allow the retrograde labeling of CeL neurons. For the injection of viruses, we injected 0.3–0.8 μl of viral solution (~10^{12} virus molecules/ml) bilaterally into CeL and waited approximately 2–3 weeks to allow maximal viral expression.

Preparation of acute brain slices and electrophysiology

Experiments were always performed on interleaved naïve and fear-conditioned animals. ice were anaesthetized with isoflurane, decapitated, and their brains quickly removed and chilled in ice-cold dissection buffer (110.0 mM choline chloride, 25.0 mM $NaHCO_3$, 1.25 mM NaH_2PO_4, 2.5 mM KCl, 0.5 mM $CaCl_2$, 7.0 mM $MgCl_2$, 25.0 mM glucose, 11.6 mM ascorbic acid and 3.1mM pyruvic acid, gassed with 95% O_2 and 5% CO_2). Coronal slices (300 μm) containing the amygdaloid complex were cut in dissection buffer by using a HM650 Vibrating Microtome (MICROM International GmbH, Walldorf, Germany), and subsequently transferred to a storage chamber containing artificial cerebrospinal fluid (ACSF) (118 mM NaCl, 2.5 mM KCl, 26.2 mM $NaHCO_3$, 1 mM NaH_2PO_4, 20 mM glucose, 2 mM $MgCl_2$ and 2 mM $CaCl_2$, at 34 °C, pH 7.4, gassed with 95% O_2 and 5% CO_2). After at least 40 min recovery time, slices were transferred to room temperature and were constantly perfused with ACSF.

In acute slices the major subdivisions of the amygdala can be easily identified under trans-illumination[23,48]. In addition, we took advantage of the SOM-Cre/Ai14 line, in which the CeL had very high density of SOM^+ neurons that are red fluorescent (Fig. 1a, Supplementary Fig. 1a–c), to facilitate the identification of CeL under epifluorescence illumination.

Simultaneous whole-cell patch-clamp recordings from SOM^+/SOM^- neuronal pairs in CeL were obtained with Multiclamp 700B amplifiers (Molecular Devices, Sunnyvale, CA, USA). Recordings were under visual guidance using an Olympus BX51 microscope equipped with both transmitted light illumination and epifluorescence illumination. The SOM^+ cells were identified based on their red-fluorescence from tdTomato. For evoked EPSCs, synaptic responses were evoked with a bipolar stimulating electrode placed in the LA approximately 0.2 mm away from the recorded cell bodies in CeL. Electrical stimulation was delivered every 30 seconds and synaptic responses were low-pass filtered at 1 KHz and recorded at holding potentials of −70 mV (for AMPA-receptor-mediated responses), +40 mV (for NMDA-receptor-mediated responses), or 0 mV (for GABA-A-receptor-mediated responses). NMDA-receptor-mediated responses were quantified as the mean current between 110 ms and 160 ms after stimulation. Recordings were performed in the ACSF. The internal solution for voltage-clamp experiments contained 115 mM caesium methanesulphonate, 20 mM CsCl, 10 mM HEPES, 2.5 mM $MgCl_2$, 4 mM Na_2-ATP, 0.4 mM Na_3GTP, 10 mM Na-phosphocreatine and 0.6 mM EGTA (pH 7.2). For current-clamp experiments the internal solution consisted of 130 mM potassium gluconate, 5 mM KCl, 10 mM HEPES, 2.5 mM $MgCl_2$, 4 mM Na_2ATP, 0.4 mM Na_3GTP, 10 mM Na-phophocreatine, and 0.6 mM EGTA (pH 7.2). Evoked EPSCs were recorded with picrotoxin (100 μM) added to the ACSF. mEPSCs were recorded in the presence of tetrodotoxin (TTX; 1 μM) and picrotoxin (100 μM). Electrophysiological data were acquired and analyzed using pCLAMP 10 software (Molecular Devices). mEPSCs were analyzed using Mini Analysis Program (Synaptosoft, Inc., Decatur, GA, USA).

To evoke synaptic transmission using ChR2, we used a single-wavelength LED system (λ = 470 nm; CoolLED.com) connected to the epifluorescence port of the Olympus BX51 microscope. To restrict the size of the light beam for focal stimulation, a built-in shutter along the light path in the BX51 microscope was used. The smallest light beam achieved using this method is ~50 μm in diameter. Light pulses of 2 ms, triggered by a TTL signal from the Clampex software (Molecular Devices), were used to evoke synaptic transmission. To measure Arch mediated neuronal inhibition, a CBT-40 Green LED (λ = 530 nm; Luminus Devices, Inc., Billerica, MA, USA) was used.

In vivo optogenetic and chemical-genetic manipulations

For *in vivo* optogenetic manipulations in awake behaving animals, *SOM-IRES-Cre* mice were bilaterally implanted with optical fiber cannulae (Doric lenses) during the same surgery procedure for viral injection. Optical fibers (100 μm in diameter) were placed 0.5 mm dorsal to the virus injection site, and were secured to the skull with C&B-Metabond Quick adhesive luting cement (Parkell Prod Inc.) followed by dental cement (Lang Dental Manufacturing, Co.). Viruses were allowed to express for 2–3 weeks. The optic fibers were connected to a laser source using an optic fiber sleeve (Doric Lenses), and the mice were subjected to behavioral tests after habituation. Naïve mice that were injected with the ChR2 virus, or a control virus that expresses GFP, into CeL were tested for freezing behavior upon the delivery of blue light pulses (λ = 473 nm, OEM Laser Systems, Inc.) through the optic fibers to activate ChR2. The light stimuli were 5-ms light pulses delivered at 50 Hz for 20 s, and were repeated 5 times with a 2-min inter-train-interval. Freezing behavior was measured

during a 20-s period immediately before the delivery of light pulses (light off), and the 20-s period of light presentation (light on; see Fig. 7c). Mice injected with the Arch virus, or a control virus that expresses GFP, were first trained with the fear-conditioning paradigm, and were then tested for conditioned fear expression 24 h later as described above. We measured the conditioned freezing behavior in response to two 20-s tones, the first of which was presented during the delivery of a constant green light (λ = 532 nm, OEM Laser Systems, Inc., Salt Lake City, USA) through the optic fibers to activate Arch (see Fig. 7e). The power of both the blue and green lasers was 5–10 mW measured at the tip of the optic fiber.

For the chemical-genetic manipulation, *SOM-IRES-Cre* mice that received bilateral injections of either the AAV-DIO-hM4Di-mCherry or the AAV-DIO-GFP (a control virus) into CeL were intraperitoneally (i.p.) injected with CNO (10 mg/kg), 40 min later followed by fear conditioning. Besides a standard conditioning procedure (Fig. 4c, d; Supplementary Fig. 2; Supplementary Fig. 5c), we also used a mild procedure (Fig. 4e, f) in which the 4-kHz tones, each co-terminating with a 2-s 0.3-mA foot-shock, were delivered twice at an interval of 120 s. This was to increase our ability to detect an effect of the manipulation on fear memory by avoiding potential compensation due to overtraining[9].

Statistics and data presentation

We used a bootstrap procedure, which makes no assumptions on the data's distribution, to compare the means of data sets with non-normal distribution that was determined by the Shapiro-Wilk test. Two data sets (*N* of size *n* with mean *Nm* and *M* of size *m* with mean *Mm*) were randomly sampled *n* and *m* times, respectively, allowing resampling, and means, *Ni* and *Mi*, were generated respectively. This procedure was repeated 10,000 times. If *Nm* was greater than *Mm, it was* considered significant if *Mi* was greater than *Ni* less than 5% of the time, for $P < 0.05$, or 1% of the time, for $P < 0.01$. All other statistical tests are indicated when used. The sample sizes used in this study, such as the numbers of cells or animals, are about the same as those estimated by power analysis (power = 0.9, $\alpha = 0.05$). No animals or data points were excluded from analysis. All data are presented as mean ± s.e.m.

Supplementary Material

Refer to Web version on PubMed Central for supplementary material.

Acknowledgments

We thank R.H. Paik for expert technical assistance, K. Deisseroth and M. Mirrione for the initial help with optogenetic methods, M.M. Luo and S.H. Shi for the *AAV-DIO-hM4Di-mCherry* construct, W. Wei for help with the focal optogenetic stimulation, A. Zador for sharing the AAV-DIO-ChR2(H134R)-YFP and AAV-DIO-Arch-GFP viruses and A. Reid for sharing the *Ai32* mice, and K. Pradhan for advice on statistic analysis. We thank S. Shea, L. Van Aelst, and R. Malinow for critical reading of the manuscript, and members of the Li Lab for discussions. This study was supported by NIH (B.L. and Z.J.H.), the Dana Foundation (B.L.), and NARSAD (B.L. and Z.J.H.).

References

1. LeDoux JE. Emotion circuits in the brain. Annual review of neuroscience. 2000; 23:155–84.
2. Davis, M. The role of the amygdala in conditioned and unconditioned fear and anxiety. In: Aggleton, JP., editor. The Amygdala. Oxford UP; Oxford: 2000. p. 213-287.

3. Davis M, Whalen PJ. The amygdala: vigilance and emotion. Molecular Psychiatry. 2001; 6:13–34. [PubMed: 11244481]
4. Maren S, Quirk GJ. Neuronal signalling of fear memory. Nature reviews Neuroscience. 2004; 5:844–52. [PubMed: 15496862]
5. LeDoux J. The amygdala. Current biology: CB. 2007; 17:R868–74. [PubMed: 17956742]
6. Ehrlich I, et al. Amygdala inhibitory circuits and the control of fear memory. Neuron. 2009; 62:757–71. [PubMed: 19555645]
7. Sigurdsson T, Doyere V, Cain CK, LeDoux JE. Long-term potentiation in the amygdala: a cellular mechanism of fear learning and memory. Neuropharmacology. 2007; 52:215–27. [PubMed: 16919687]
8. Johansen JP, Cain CK, Ostroff LE, LeDoux JE. Molecular mechanisms of fear learning and memory. Cell. 2011; 147:509–24. [PubMed: 22036561]
9. Rumpel S, LeDoux J, Zador A, Malinow R. Postsynaptic receptor trafficking underlying a form of associative learning. Science. 2005; 308:83–8. [PubMed: 15746389]
10. Clem RL, Huganir RL. Calcium-permeable AMPA receptor dynamics mediate fear memory erasure. Science. 2010; 330:1108–12. [PubMed: 21030604]
11. Quirk GJ, Repa C, LeDoux JE. Fear conditioning enhances short-latency auditory responses of lateral amygdala neurons: parallel recordings in the freely behaving rat. Neuron. 1995; 15:1029–39. [PubMed: 7576647]
12. Rogan MT, Staubli UV, LeDoux JE. Fear conditioning induces associative long-term potentiation in the amygdala. Nature. 1997; 390:604–7. [PubMed: 9403688]
13. McKernan MG, Shinnick-Gallagher P. Fear conditioning induces a lasting potentiation of synaptic currents in vitro. Nature. 1997; 390:607–11. [PubMed: 9403689]
14. Goosens KA, Maren S. Pretraining NMDA receptor blockade in the basolateral complex, but not the central nucleus, of the amygdala prevents savings of conditional fear. Behavioral neuroscience. 2003; 117:738–50. [PubMed: 12931959]
15. Pare D, Quirk GJ, Ledoux JE. New vistas on amygdala networks in conditioned fear. Journal of Neurophysiology. 2004; 92:1–9. [PubMed: 15212433]
16. Wilensky AE, Schafe GE, Kristensen MP, LeDoux JE. Rethinking the fear circuit: the central nucleus of the amygdala is required for the acquisition, consolidation, and expression of Pavlovian fear conditioning. The Journal of neuroscience: the official journal of the Society for Neuroscience. 2006; 26:12387–96. [PubMed: 17135400]
17. Ciocchi S, et al. Encoding of conditioned fear in central amygdala inhibitory circuits. Nature. 2010; 468:277–82. [PubMed: 21068837]
18. Haubensak W, et al. Genetic dissection of an amygdala microcircuit that gates conditioned fear. Nature. 2010; 468:270–276. [PubMed: 21068836]
19. Duvarci S, Popa D, Pare D. Central Amygdala Activity during Fear Conditioning. Journal of Neuroscience. 2011; 31:289–294. [PubMed: 21209214]
20. Cassell MD, Freedman LJ, Shi C. The intrinsic organization of the central extended amygdala. Annals of the New York Academy of Sciences. 1999; 877:217–41. [PubMed: 10415652]
21. Cassell MD, Gray TS. Morphology of peptide-immunoreactive neurons in the rat central nucleus of the amygdala. The Journal of Comparative Neurology. 1989; 281:320–33. [PubMed: 2468696]
22. LeDoux JE, Iwata J, Cicchetti P, Reis DJ. Different projections of the central amygdaloid nucleus mediate autonomic and behavioral correlates of conditioned fear. The Journal of neuroscience: the official journal of the Society for Neuroscience. 1988; 8:2517–2529. [PubMed: 2854842]
23. Dumont EC, Martina M, Samson RD, Drolet G, Pare D. Physiological properties of central amygdala neurons: species differences. The European journal of neuroscience. 2002; 15:545–52. [PubMed: 11876782]
24. Taniguchi H, et al. A resource of Cre driver lines for genetic targeting of GABAergic neurons in cerebral cortex. Neuron. 2011; 71:995–1013. [PubMed: 21943598]
25. Madisen L, et al. A robust and high-throughput Cre reporting and characterization system for the whole mouse brain. Nature Neuroscience. 2010; 13:133–40. [PubMed: 20023653]

26. Anglada-Figueroa D, Quirk GJ. Lesions of the basal amygdala block expression of conditioned fear but not extinction. The Journal of neuroscience: the official journal of the Society for Neuroscience. 2005; 25:9680–5. [PubMed: 16237172]
27. Zhu JJ, Qin Y, Zhao M, Van Aelst L, Malinow R. Ras and Rap control AMPA receptor trafficking during synaptic plasticity. Cell. 2002; 110:443–55. [PubMed: 12202034]
28. Zhang F, Wang LP, Boyden ES, Deisseroth K. Channelrhodopsin-2 and optical control of excitable cells. Nature methods. 2006; 3:785–92. [PubMed: 16990810]
29. Pitkanen A, et al. Intrinsic connections of the rat amygdaloid complex: projections originating in the lateral nucleus. The Journal of Comparative Neurology. 1995; 356:288–310. [PubMed: 7629320]
30. Ottersen OP, Ben-Ari Y. Afferent connections to the amygdaloid complex of the rat and cat. I. Projections from the thalamus. The Journal of Comparative Neurology. 1979; 187:401–24. [PubMed: 489786]
31. Turner BH, Herkenham M. Thalamoamygdaloid projections in the rat: a test of the amygdala's role in sensory processing. The Journal of Comparative Neurology. 1991; 313:295–325. [PubMed: 1765584]
32. Zucker RS, Regehr WG. Short-term synaptic plasticity. Annual review of physiology. 2002; 64:355–405.
33. Fu Y, Shinnick-Gallagher P. Two intra-amygdaloid pathways to the central amygdala exhibit different mechanisms of long-term potentiation. Journal of Neurophysiology. 2005; 93:3012–5. [PubMed: 15618080]
34. Lopez de Armentia M, Sah P. Bidirectional synaptic plasticity at nociceptive afferents in the rat central amygdala. The Journal of Physiology. 2007; 581:961–70. [PubMed: 17379642]
35. Pape HC, Pare D. Plastic synaptic networks of the amygdala for the acquisition, expression, and extinction of conditioned fear. Physiological Reviews. 2010; 90:419–63. [PubMed: 20393190]
36. Dong S, Allen JA, Farrell M, Roth BL. A chemical-genetic approach for precise spatio-temporal control of cellular signaling. Molecular bio Systems. 2010; 6:1376–80.
37. Ferguson SM, et al. Transient neuronal inhibition reveals opposing roles of indirect and direct pathways in sensitization. Nature Neuroscience. 2011; 14:22–4. [PubMed: 21131952]
38. Huber D, Veinante P, Stoop R. Vasopressin and oxytocin excite distinct neuronal populations in the central amygdala. Science. 2005; 308:245–8. [PubMed: 15821089]
39. Madisen L, et al. A toolbox of Cre-dependent optogenetic transgenic mice for light-induced activation and silencing. Nature Neuroscience. 2012; 15:793–802. [PubMed: 22446880]
40. Zhang F, Aravanis AM, Adamantidis A, de Lecea L, Deisseroth K. Circuit-breakers: optical technologies for probing neural signals and systems. Nature reviews Neuroscience. 2007; 8:577–81. [PubMed: 17643087]
41. Zhang F, et al. Optogenetic interrogation of neural circuits: technology for probing mammalian brain structures. Nature protocols. 2010; 5:439–56. [PubMed: 20203662]
42. Barth AL, Gerkin RC, Dean KL. Alteration of neuronal firing properties after in vivo experience in a FosGFP transgenic mouse. The Journal of neuroscience: the official journal of the Society for Neuroscience. 2004; 24:6466–75. [PubMed: 15269256]
43. Chow BY, et al. High-performance genetically targetable optical neural silencing by light-driven proton pumps. Nature. 2010; 463:98–102. [PubMed: 20054397]
44. Quirk GJ, Armony JL, LeDoux JE. Fear conditioning enhances different temporal components of tone-evoked spike trains in auditory cortex and lateral amygdala. Neuron. 1997; 19:613–24. [PubMed: 9331352]
45. He M, et al. Cell-type-based analysis of microRNA profiles in the mouse brain. Neuron. 2012; 73:35–48. [PubMed: 22243745]
46. Li B, et al. Synaptic potentiation onto habenula neurons in the learned helplessness model of depression. Nature. 2011; 470:535–9. [PubMed: 21350486]
47. Kopec CD, et al. A robust automated method to analyze rodent motion during fear conditioning. Neuropharmacology. 2007; 52:228–33. [PubMed: 16926033]

48. Lopez de Armentia M, Sah P. Firing properties and connectivity of neurons in the rat lateral central nucleus of the amygdala. Journal of Neurophysiology. 2004; 92:1285–94. [PubMed: 15128752]

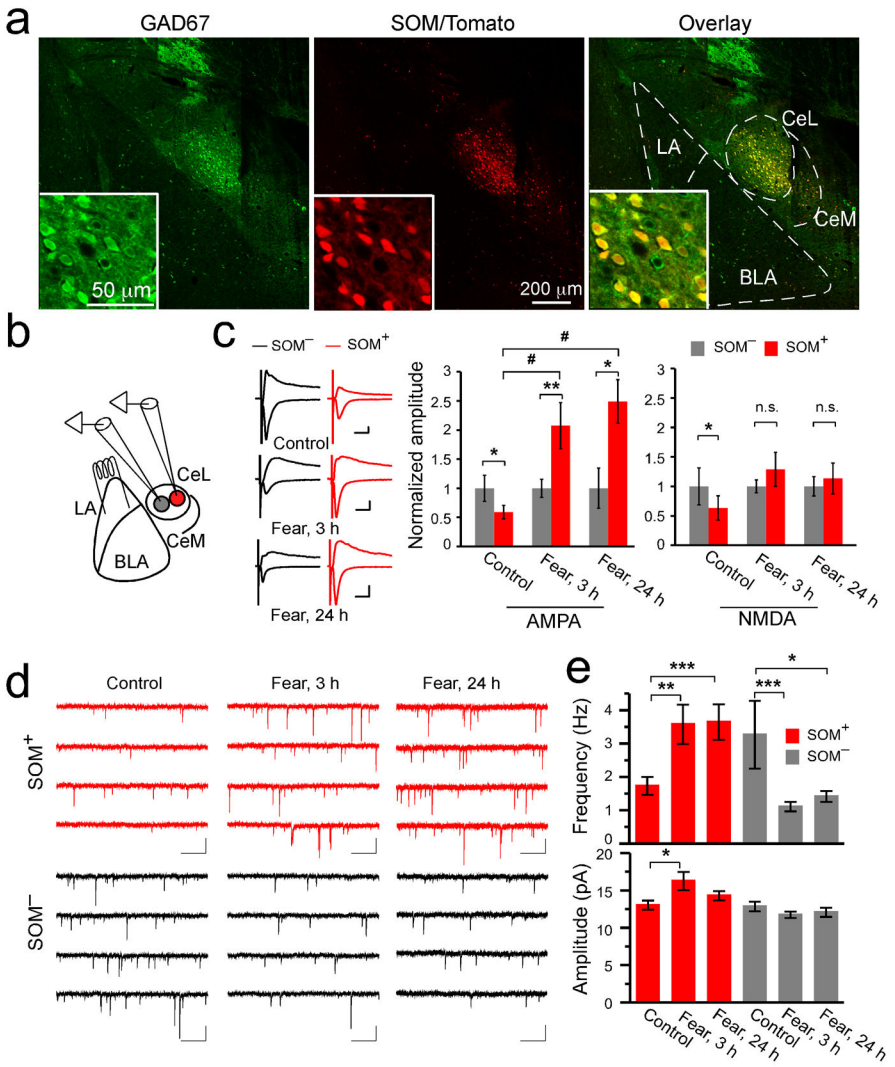

Figure 1. Fear conditioning induces modifications of excitatory synapses onto neurons in CeL

(**a**) A representative coronal brain section from the *SOM-IRES-Cre/Ai14* mice stained with anti-GAD67 antibody (left). The SOM$^+$ neurons expressed both tdTomato (middle) and GAD67 (see overlay in right). Inset: a portion of CeL shown in higher magnification. The borders of CeL, CeM, LA, and BLA are outlined. (**b**) A schematic recording configuration. In red is a SOM$^+$ neuron. (**c**) Left: representative EPSC traces recorded from SOM$^-$/SOM$^+$ neuronal pairs in CeL of the following groups: control (control group, upper panel), "fear, 3 h" (3 hrs following fear conditioning, middle panel), and "fear, 24 h" (24 hrs following fear conditioning, lower panel). Calibrations: 50 pA and 20 ms. Middle: quantification of AMPAR-mediated EPSC amplitude, which was normalized to the mean EPSC amplitude of SOM$^-$ neurons. SOM$^+$ neurons had smaller AMPAR-mediated EPSC than SOM$^-$ neurons in control animals, but this relationship was reversed in fear-conditioned animals (control: SOM$^-$, 1 ± 0.23, SOM$^+$, 0.59 ± 0.12, n =13 pairs, 4 animals, t = 2.53, DF = 12, **P* < 0.05, paired *t*-test; fear, 3 h: SOM$^-$, 1 ± 0.16, SOM$^+$, 2.07 ± 0.40, n = 11 pairs, 3 animals, t = −3.42, DF = 10, ***P*<0.01, paired *t*-test; fear, 24 h: SOM$^-$, 1±0.34, SOM$^+$, 2.49±0.37, n = 8 pairs, 2 animals, t = −2.94, DF = 7, **P* < 0.05, paired *t*-test; #*P* < 0.05, $F_{(2,29)}$ = 11.7, one-

way analysis of variance (ANOVA) followed by Tukey's test). Right: quantification of NMDAR-mediated EPSC. SOM^+ neurons had smaller NMDAR-mediated EPSC than SOM^- neurons in control animals, but this difference disappeared in fear-conditioned animals (control: SOM^-, 1 ± 0.31, SOM^+, 0.63 ± 0.20, n = 13 pairs, 4 animals, t = 2.75, DF = 12, **P* < 0.05, paired *t*-test; fear, 3 h: SOM^-, 1± 0.11, SOM^+, 1.3 ± 0.29, n = 11 pairs, 3 animals, t = −1.14, DF = 10, *P* > 0.05, paired *t*-test; fear, 24 h: SOM^-, 1 ± 0.16, SOM^+, 1.13 ± 0.26, n = 7 pairs, 2 animals, t = −0.40, DF = 6, *P* > 0.05, paired *t*-test; n.s., non-significant). (**d**) Representative mEPSC traces recorded from SOM^+ (red) and SOM^-(black) neurons in the CeL of different groups. Calibrations: 20 pA and 500 ms. (**e**) Upper panel: fear conditioning increased the mEPSC frequency of SOM^+ neurons (SOM^+, control: 1.73 ± 0.27 Hz, n = 15 cells, 3 animals; fear, 3 h: 3.58 ± 0.59 Hz, n = 15 cells, 3 animals; fear, 24 h: 3.64 ± 0.53 Hz, n = 12 cells, 3 animals; **P* < 0.05, ***P* < 0.01, ****P* < 0.001, bootstrap with Bonferroni correction), while decreased that of SOM^- neurons (SOM^-, control: 3.26 ± 1.02 Hz, n = 12 cells, 3 animals; fear, 3 h: 1.11 ± 0.14 Hz; n = 10 cells, 3 animals; fear, 24 h: 1.42 ± 0.16 Hz, n = 13 cells, 3 animals; **P* < 0.05, ****P* < 0.001, bootstrap with Bonferroni correction). Lower panel: fear conditioning increased the mEPSC amplitude of SOM^+ neurons at 3 hrs after fear conditioning (SOM^+, control: 13.03 ± 0.60 pA, n = 15 cells, 3 animals; fear, 3 h: 16.26 ± 1.21 pA, n = 15 cells, 3 animals; fear, 24 h: 14.28 ± 0.63 Hz, n = 12 cells, 3 animals; **P* < 0.05, bootstrap with Bonferroni correction), but did not affect that of SOM^- neurons (SOM^-, control: 12.85 ± 0.64 pA, n = 12 cells, 3 animals; fear, 3 h: 11.74 ± 0.44 pA, n = 10 cells, 3 animals; fear, 24 h: 12.06 ± 0.61 Hz, n = 13 cells, 3 animals; *P* > 0.05, bootstrap). Fear, fear-conditioned. Error bars, s.e.m.

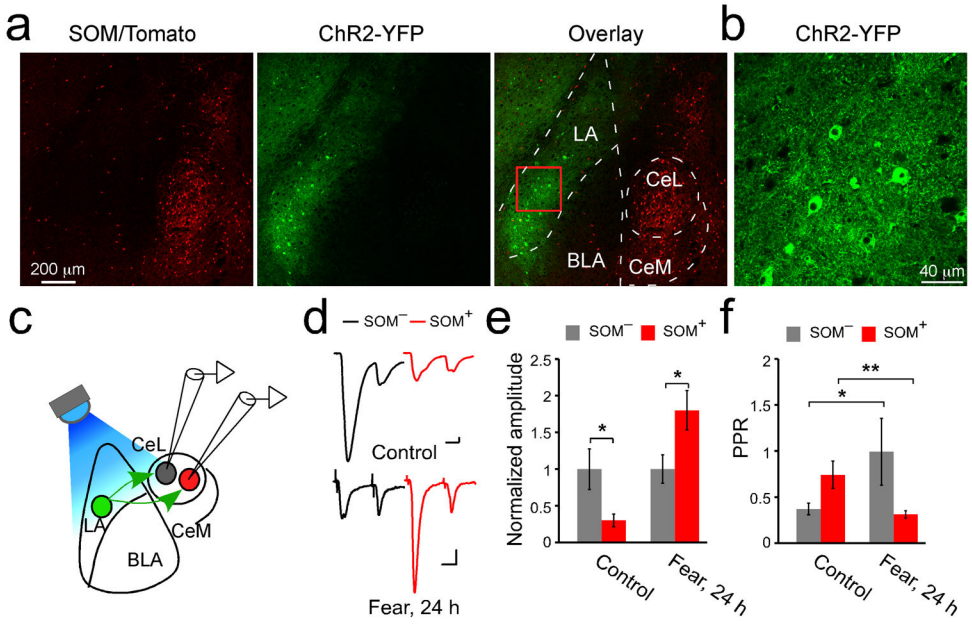

Figure 2. The fear conditioning-induced synaptic modifications in CeL are expressed presynaptically at the LA-CeL pathway

(**a**) Confocal images of a coronal brain section, which was recovered after electrophysiological recording (see **c**, **d**), from a *SOM-IRES-Cre/Ai14* mouse injected with the AAV-CAG-ChR2(H134R)-YFP into the LA (middle). The SOM^+ neurons expressed tdTomato (left, and overlay in right). The borders of CeL, CeM, LA, and BLA are outlined. (**b**) ChR2-YFP is expressed in many LA neurons. A higher magnification image of the boxed region in **a** (see overlay) is shown. (**c**) A schematic recording configuration. In green is a ChR2-YFP-positive neuron in LA, in red a SOM^+ neuron in CeL. A blue LED (λ = 470 nm) was used to activate ChR2 and evoke the LA neuron-driven synaptic transmission, which is simultaneously recorded from SOM^-/SOM^+ neuronal pairs in CeL. (**d**) Representative EPSCs, which were evoked by light stimulation of the LA–CeL pathway, were recorded from SOM^-/SOM^+ neuronal pairs in the CeL, in control (upper panel) and "fear, 24 h" (24 hrs following fear conditioning, lower panel) groups. A paired-pulse stimulation protocol (50 ms inter-event-interval) was used. Calibrations: 20 pA and 20 ms. (**e**) Quantification of AMPAR-mediated EPSC amplitude (peak of the EPSC in response to the first pulse in the paired-pulse), which was normalized to the mean EPSC amplitude of SOM^- neurons. SOM^+ neurons had smaller EPSC than SOM^- neurons in control animals (control: SOM^-, 1 ± 0.28, SOM^+, 0.3 ± 0.08, n =14 pairs, 2 animals; t = 2.98, DF = 13, **P* < 0.05, paired *t*-test), but this relationship was reversed in fear-conditioned animals (fear, 24 h: SOM^-, 1 ± 0.19, SOM^+, 1.8 ± 0.27, n = 28 pairs, 3 animals; t = −2.42, DF = 27, **P*<0.05, paired *t*-test). (**f**) Quantification of PPR. SOM^- neurons increased, whereas SOM^+ neurons decreased PPR after fear conditioning (SOM^-, control: 0.37 ± 0.06, n = 14 cells, 2 animals, fear, 24 h: 0.99 ± 0.36, n = 22 cells, 3 animals; **P* < 0.05, bootstrap; SOM^+, control: 0.74 ± 0.15, n =11 cells, 2 animals, fear, 24 h: 0.31 ± 0.04, n = 26 cells, 3 animals; ***P* < 0.01, bootstrap). Error bars, s.e.m.

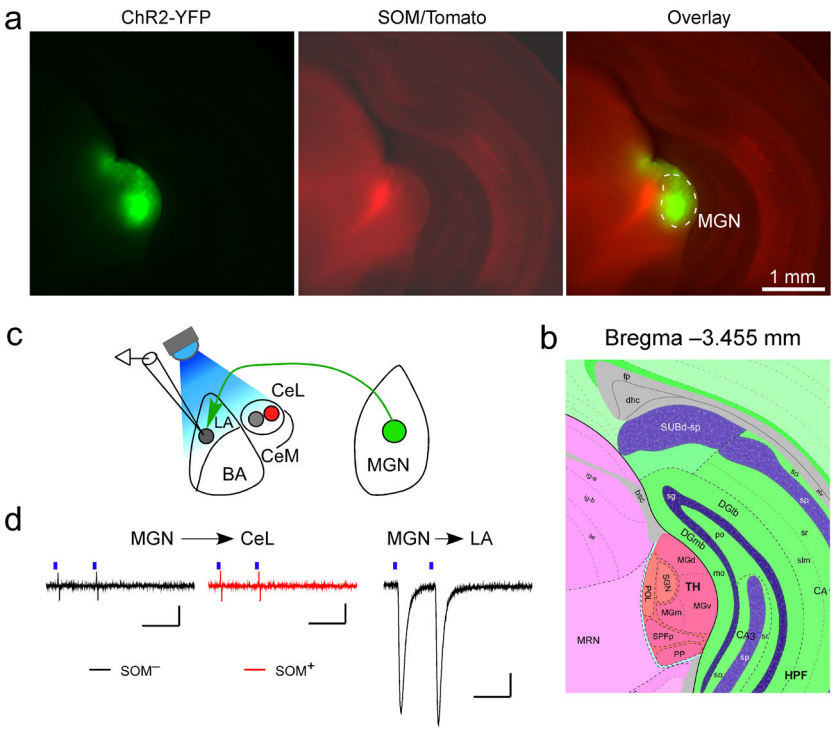

Figure 3. Auditory thalamus does not drive excitatory synaptic transmission onto CeL neurons

(**a**) Images of a coronal brain section, which was recovered from a brain used for making acute slices for recording (see **c**, **d**), from a *SOM-IRES-Cre/Ai14* mouse injected with AAV-CAG-ChR2(H134R)-YFP into the medial geniculate nucleus (MGN) (left, and overlay in the right). Images were taken using an Olympus BX41 histology microscope with a 5x lens. Note the area infected with the virus was large and covered the entire MGN (see **b**) for the atlas). (**b**) A section of a brain atlas that contains the auditory thalamus, which is at Bregma −3.455 mm, a level approximately the same as that of the brain section shown in **a**. The atlas is adapted from the mouse Reference Atlas of Allen Brain Institute. (**c**) A schematic recording configuration. In green is a ChR2-positive neuron in MGN, in red a SOM^+ neuron in CeL. (**d**) Left: representative EPSC traces recorded from a SOM^- (black) and a SOM^+ (red) neuron in the CeL. Out of 11 SOM^- (2 animals) and 11 SOM^+ (2 animals) neurons recorded in CeL, none had any measurable EPSCs. Right: a representative EPSC trace recorded from an LA neuron in the same slice as that used in the left. EPSCs could be readily evoked for all 17 neurons (2 animals) recorded in LA (EPSC amplitude: 154.2 ± 36.6 pA, mean±s.e.m.). Blue bars indicate light pulses (2 ms). Calibrations: 20 pA and 50 ms.

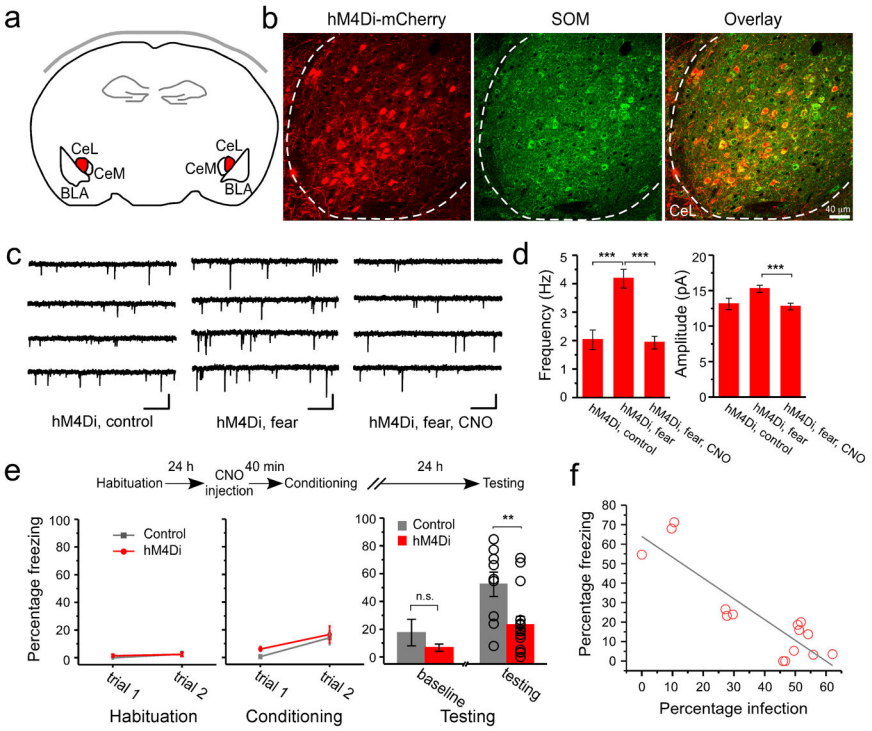

Figure 4. Synaptic potentiation onto SOM$^+$ neurons in CeL is required for the formation of fear memory

The *SOM-IRES-Cre* mice were used in these experiments. (**a**) A schematic experimental design. The hM4Di-mCherry is expressed in SOM$^+$ neurons in CeL (shown in red) by viral infection. (**b**) An example image of the SOM$^+$ neurons in CeL infected with the AAV-DIO-hM4Di-mCherry virus. Left: expression of hM4Di (red) was detected based on the intrinsic fluorescence of mCherry. Middle: SOM$^+$ neurons (green) were recognized by an antibody against SOM. Right: Only SOM$^+$ neurons expressed hM4Di, as indicated by the overlapping of red and green signals. Dashed lines mark the border of CeL. Coronal sections. (**c**) Representative mEPSC traces recorded from SOM$^+$ CeL neurons expressing hM4Di-mCherry, in the following groups: “hM4Di, control” (control), “hM4Di, fear” (fear conditioning), and “hM4Di, fear, CNO” (fear conditioning with CNO pre-treatment). For the fear conditioning groups, acute brain slices were prepared 3 hr following fear conditioning. Calibrations: 20 pA and 500 ms. (**d**) Left: CNO pre-treatment suppressed the fear conditioning-induced increase in mEPSC frequency in SOM$^+$ neurons that expressed hM4Di (control: 2.02 ± 0.35 Hz, n = 11 cells, 3 animals; fear: 4.18 ± 0.33 Hz, n = 15 cells, 3 animals; fear, CNO: 1.93 ± 0.22 Hz, n = 12 cells, 3 animals; ***P < 0.001, bootstrap with Bonferroni correction). Right: CNO pre-treatment also suppressed the fear conditioning-induced increase in mEPSC amplitude in SOM$^+$ neurons that expressed hM4Di (control: 13.1 ± 0.81 Hz, n = 11 cells, 3 animals; fear: 15.24 ± 0.51 Hz, n = 15 cells, 3 animals; fear, CNO: 12.75 ± 0.47 Hz, n = 12 cells, 3 animals; ***P < 0.001, bootstrap with Bonferroni correction). (**e**) Top: A schematic experimental procedure. Bottom left & middle: freezing behavior during habituation and conditioning. Control: *SOM-IRES-Cre* mice that received AAV-DIO-GFP injection bilaterally into CeL. hM4Di: *SOM-IRES-Cre* mice that received AAV-DIO-hM4Di injection bilaterally into CeL. Freezing responses were similar for the

two groups at the end of conditioning (control, 14.2 ± 4.9%, n = 9 animals; hM4Di, 16.6 ± 6.1%, n = 15 animals; $P > 0.05$, *t*-test). Bottom right: the hM4Di mice showed impaired fear memory recall compared with control (control, 52.36 ± 8.76%, n = 9 animals; hM4Di, 23.24 ± 6.05%, n = 15 animals; t = 2.82, DF = 22, $^{**}P < 0.01$, *t*-test). The two groups did not differ significantly in their baseline freezing levels (control, 17.56 ± 9.62%, n = 9 animals; hM4Di, 6.67 ± 2.37%, n = 15 animals; $P > 0.05$, *t*-test). (**f**) The freezing level of individual animals correlated with the extent of infection, measured as the fraction of SOM^+ CeL neurons that expressed hMD4i-mCherry ($R^2 = 0.76$, $F_{(1,13)} = 45.62$, grey line; $P < 0.001$ by a linear regression; n = 15 animals). The extent of infection for the left and right CeL was averaged. Error bars, s.e.m.

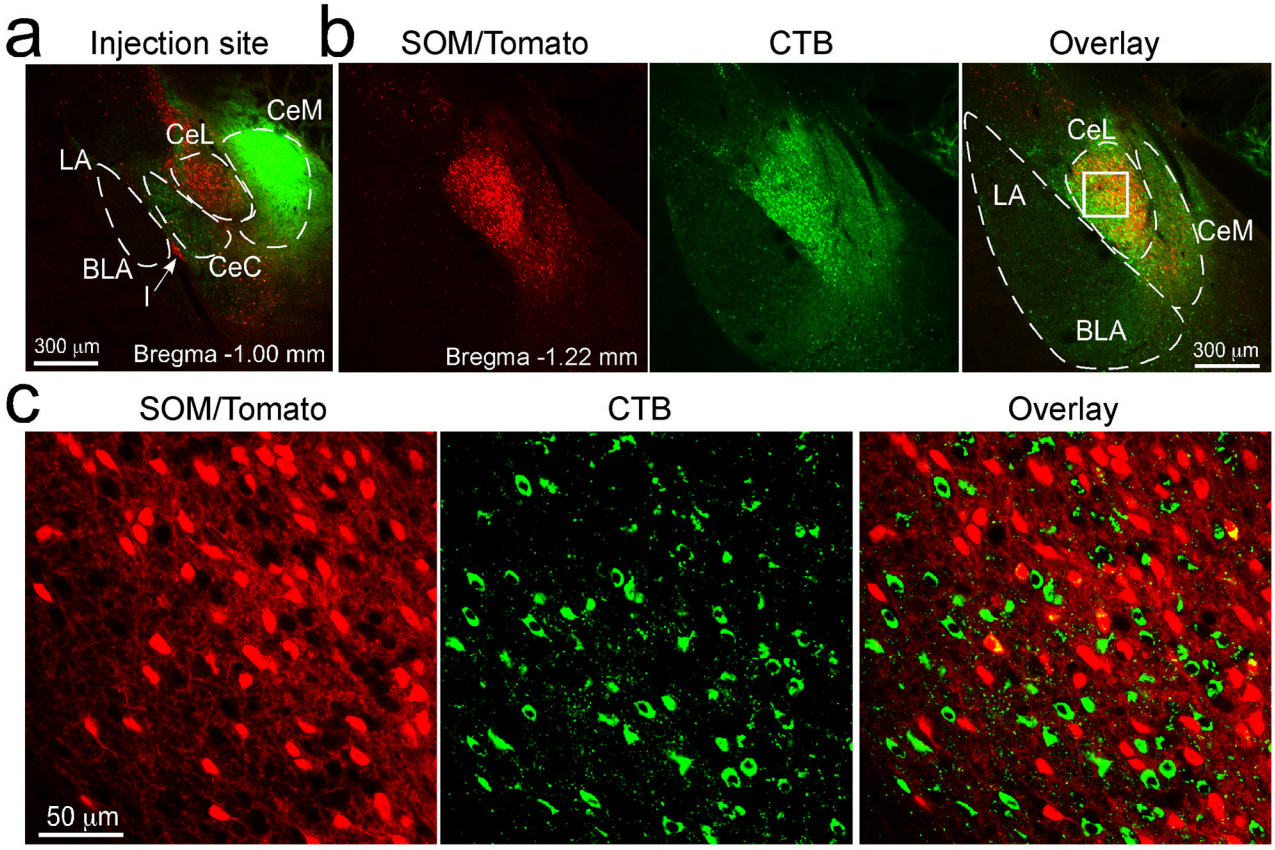

Figure 5. SOM$^+$ CeL neurons do not project to CeM

(**a**) CTB (green) was injected into the CeM of a *SOM-IRES-Cre/Ai14* mouse (similar results were obtained from 2 animals). Coronal brain section (at ~Bregma −1.00 mm). (**b**) Images of a brain section from the same mouse (at ~Bregma −1.22 mm). Left, the SOM$^+$ neurons expressed tdTomato (red). Middle, extensive labeling by CTB (green) was seen in CeL. Right, overlay; the box in CeL marks the region shown in **c** at higher magnification. (**c**) Higher magnification images of the boxed region in CeL in **b**. The vast majority of the CTB-labeled neurons (green) in CeL were not SOM$^+$ (red; see overlay in right).

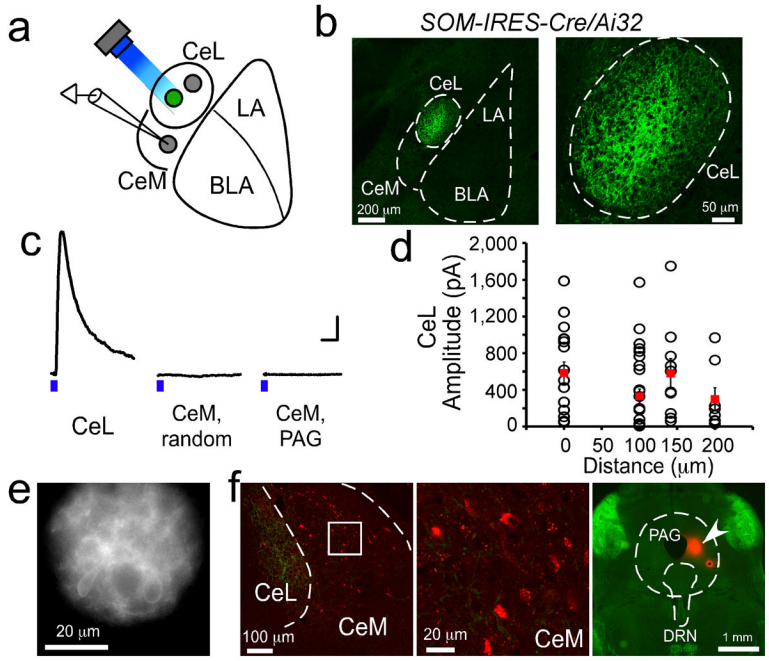

Figure 6. SOM$^+$ CeL neurons do not inhibit CeM neurons that project to PAG

(**a**) A schematic recording configuration. In green is a SOM$^+$ neuron that expresses ChR2-YFP. Recordings were made onto CeL or CeM neurons that did (SOM$^+$ cells) or did not (SOM$^-$ cells) express ChR2-YFP. Holding potential was set at 0 mV, which is the reversal potential of ChR2. A blue LED (λ = 470 nm), the beam size of which was restricted to ~50 μm in diameter by a shutter (see **e**), was used to activate ChR2-expressing cells in multiple locations that together covered the entire CeL. (**b**) A coronal brain section from a *SOM-IRES-Cre/Ai32* mouse, in which the ChR2-YFP was specifically and uniformly expressed in SOM$^+$ cells. Prominent labeling with ChR2-YFP was seen in cell bodies and fibers in CeL. Weak labeling of fibers was occasionally observed in CeM. On the right is a higher magnification image of the CeL area. (**c**) Representative IPSC traces recorded from a CeL neuron, a randomly recorded CeM neuron (CeM, random), and a PAG-projecting CeM neuron (CeM, PAG), respectively. IPSCs were evoked by 2-ms light pulses (denoted by the blue bars) from an LED set at a constant power for all recordings. Calibrations: 100 pA and 50 ms. (**d**) Quantification of the amplitude of IPSCs in CeL neurons in response to the focal stimulation of SOM$^+$ cells in different locations of CeL. X-axis is the distances (in μm) between the soma of the recorded cells and the center of stimulation. Each circle represents an IPSC of one cell in response to the stimulation of one location (red squares: mean ± s.e.m, n = 17 cells, 3 animals). All neurons recorded in CeL showed robust IPSCs for all stimulation locations. In contrast, only 4 out of 40 randomly recorded CeM cells (from 3 animals) had measurable IPSCs (not shown), while none (0 out of 16 cells, 1 animal) of the PAG-projecting CeM cells showed any measurable IPSCs. (**e**) An image showing the field of illumination by the LED light beam used for the light stimulation in CeL. The ChR2-YFP-expressing cells are clearly visible. (**f**) Left: image of a coronal brain section containing CeM. The brain section was prepared from a *SOM-IRES-cre/Ai32* mouse, in which the CTB conjugated to the dye Alexa Fluor 594 was injected into the PAG. Middle: the boxed region

in CeM is shown in higher magnification. The CTB-labeled PAG-projecting neurons are red fluorescent. Right: an image of the brain section containing PAG. Arrowhead indicates the site of CTB injection. DRN: dorsal raphe nucleus. Error bars, s.e.m.

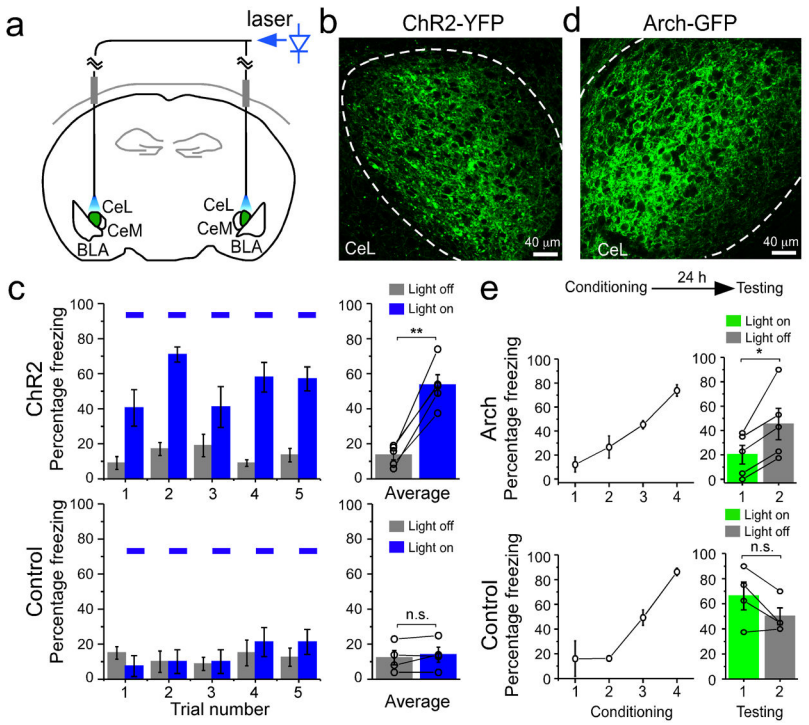

Figure 7. SOM$^+$ neurons in CeL control the expression of fear

The *SOM-IRES-Cre* mice were used in these experiments. (**a**) A schematic diagram showing the experimental design. ChR2-YFP (or Arch-GFP) was expressed in SOM$^+$ neurons in CeL (shown in green) by viral infection. Optic fibers were chronically implanted bilaterally in CeL, and were connected to a blue (for ChR2 activation) or a green (for Arch activation, not shown) laser source. (**b**) An example image of the SOM$^+$ neurons in CeL infected with the AAV-DIO-ChR2(H134R)-YFP virus. Dashed lines mark the border of CeL. (**c**) Activation of SOM$^+$ CeL neurons induced fear-like responses in naïve animals. Left: freezing behavior was measured, in repeated trials, before and during the delivery of blue light pulses (blue bars) into the CeL. Delivery of light into CeL induced freezing behavior in animals injected with the AAV-DIO-ChR2(H134R)-YFP virus (ChR2 group, top), but not in animals injected with the AAV-GFP virus (Control group, bottom). Right: level of freezing was averaged for ChR2 animals (top; light off, 13.50 ± 2.63%, light on, 53.50 ± 5.90%, n = 5 animals, t = −7.95, DF = 4, $^{**}P < 0.01$, paired *t*-test) and control animals (bottom; light off, 12.25 ± 4.13%, light on, 14.00 ± 4.30%, n = 4 animals, t = −1.13, DF = 3, $P > 0.05$, paired *t*-test). (**d**) An example of the SOM$^+$ neurons in CeL infected with the AAV-DIO-Arch-GFP. Dashed lines mark the border of CeL. (**e**) Inhibition of SOM$^+$ CeL neurons suppressed conditioned fear expression. Top: a schematic experimental procedure, in which animals were first trained with the fear-conditioning paradigm, and 24 h later tested for fear memory recall. Middle and Bottom panels: animals injected with the AAV-DIO-Arch-GFP (Arch group, middle) or the AAV-GFP virus (Control group, bottom) were fear conditioned (left) and then tested (right). During testing, conditioned freezing was measured in two trials, the first of which was conducted during the delivery of a green light into CeL (light on). Delivery of light into CeL suppressed conditioned freezing in the Arch group (light on: 20.20 ± 7.69%, light off: 45.3 ± 12.91%, n = 5 animals, t = −3.72, DF = 4, $^{*}P < 0.05$, paired

t-test), but not in the control group (light on, 66.25 ± 11.11%, light off, 50.00 ± 6.77%, n = 4 animals, t = 2.39, DF = 3, $P > 0.05$, paired *t*-test). n.s. not significant, Error bars, s.e.m.